

Research Article

An Adaptive Channel Model for VBLAST in Vehicular Networks

Ghassan M. T. Abdalla,¹ Mosa A. Abu-Rgheff,¹ and Sidi-Mohammed Senouci²

¹ School of Computing Communications and Electronics, University of Plymouth, Plymouth, PL4 8AA Devon, UK

² Orange Labs CORE/M2I, 2 Avenue Pierre Marzin, 22307 Lannion Cedex, France

Correspondence should be addressed to Ghassan M. T. Abdalla, ghassan.abdalla@plymouth.ac.uk

Received 6 May 2008; Revised 16 October 2008; Accepted 1 February 2009

Recommended by Weidong Xiang

The wireless transmission environment in vehicular ad hoc systems varies from line of sight with few surroundings to rich Rayleigh fading. An efficient communication system must adapt itself to these diverse conditions. Multiple antenna systems are known to provide superior performance compared to single antenna systems in terms of capacity and reliability. The correlation between the antennas has a great effect on the performance of MIMO systems. In this paper we introduce a novel adaptive channel model for MIMO-VBLAST systems in vehicular ad hoc networks. Using the proposed model, the correlation between the antennas was investigated. Although the line of sight is ideal for single antenna systems, it severely degrades the performance of VBLAST systems since it increases the correlation between the antennas. A channel update algorithm using single tap Kalman filters for VBLAST in flat fading channels has also been derived and evaluated. At 12 dB E_s/N_0 , the new algorithm showed 50% reduction in the mean square error (MSE) between the actual channel and the corresponding updated estimate compared to the MSE without update. The computational requirement of the proposed algorithm for a $p \times q$ VBLAST is $6p \times q$ real multiplications and $4p \times q$ real additions.

Copyright © 2009 Ghassan M. T. Abdalla et al. This is an open access article distributed under the Creative Commons Attribution License, which permits unrestricted use, distribution, and reproduction in any medium, provided the original work is properly cited.

1. Introduction

Crash prevention, road traffic control, route guidance, internet on the road as well as multimedia services, and others are the promising applications of vehicular ad hoc networks (VANET). Such applications require high data rates and high reliability with minimum human interaction. Although the technology used in wireless communication such as IEEE 802.11 has reached a high level of maturity and is capable of providing high bit rates, its performance in high speed transmission and adaptability to channel conditions ranging from strong line of sight to Rayleigh fading are of concern. Multiple-input multiple-output (MIMO) systems, including diversity, space-time coding, and BLAST algorithms, have been thoroughly studied and have shown superior performance [1] compared to single antenna systems for mobile communications in rich scattering, no line of sight, and slowly varying channel conditions. However, the conditions are different in VANET, and an accurate channel model is required to study the performance of MIMO systems. Moreover, since MIMO algorithms require accurate channel state information, the issue of channel tracking is raised.

In this paper, we adapt the elliptical model introduced in [2] to simulate the MIMO channel in VANET. The channel Doppler spectrum was calculated and compared to that of the classical Jakes model [3]. As will be shown, the Doppler spectrum is different from that of Jakes' model due to the movement of the scatterers. The correlation between antennas was also studied under various line of sight conditions. The results show that an antenna separation of 3λ or more, λ represents the wavelength, can achieve a correlation less than 0.5 unless a very strong line of sight exists. A novel channel update algorithm to track the channel is then introduced. The new algorithm improves the bit error rate (BER) performance of MIMO systems with a minor increase in hardware complexity.

The paper is organised as follows. Some of the existing models and their applications are discussed in the next section. Section 3 is a detailed description of the proposed channel model. In Section 4, a comparison between the proposed model and Jakes' model is provided as well as correlation results for a broadside antenna array. The channel update algorithm is derived and assessed in Section 5. Finally, Section 6 concludes the paper.

2. An Overview of Existing Channel Models

Several models have been developed to approximate the mobile wireless channel. The main parameters in designing a channel model are the heights of transmit and receive antennas, the position of the surroundings relative to the antennas, the Doppler spectrum as well as the parameters intended for calculation. The early work on wireless channel modelling showed that the envelope of the received signal has a Rician distribution and becomes Rayleigh distributed when no line of sight exists [4]. The well-known Jakes analysis showed that the autocorrelation ($R(\tau)$) and Doppler power spectrum ($P(f)$) of the channel are given by [3]

$$R(\tau) = J_0(2\pi f_D \tau),$$

$$P(f) = \begin{cases} \frac{1}{\pi f_D} \frac{1.5}{\sqrt{1 - (f/f_D)^2}}, & |f| < f_D, \\ 0, & \text{otherwise,} \end{cases} \quad (1)$$

$$f_D = \frac{v}{\lambda},$$

where f_D is the maximum Doppler shift, v is the relative transmitter receiver speed, and J_0 is the zero-order Bessel function.

To simulate the received signal at a mobile terminal from a basestation, or vice versa, in macrocells, Lee's model is usually used [5]. Since the basestation is positioned over high buildings, the number of surroundings is small, while for a mobile terminal at street level, a large number of surroundings are available. Therefore, Lee modelled the channel by a ring of scatterers uniformly distributed around the terminal which affects both the terminal and basestation [6]. Lee's model was extended to model ad hoc networks in [7]. Since in ad hoc networks the transmitter and receiver are usually peers, both are assumed to be surrounded by scatterers; therefore, the authors of [7] developed a two-ring model which uses one ring of scatterers around the transmitter and another around the receiver. The two-ring model was extended to three dimensions in [8] to study the performance of vertical antenna arrays. The three-dimensional model assumes that the terminals are surrounded by scatterers of various heights, and the authors used cylinders instead of rings to model the channel. An elliptical model was introduced in [2] to study the angle of arrival (AOA) and angle of departure (AOD) as well as the performance of antenna arrays at basestations in microcells. Basestations in microcells are at street lights heights and, therefore, are more affected by the surroundings than those in macrocells. The probability of line of sight communication in microcells is also much greater than in macrocells. The model places the transmitter and receiver at the foci of an ellipse. The two-ring and three-dimensional channel models are ideal for urban areas under heavy traffic conditions where there are a large number of surroundings and no line of sight. However, in suburban areas, open areas, or light traffic conditions, the assumptions of large number of surroundings and no line of sight become invalid and, therefore, a more realistic channel model is required.

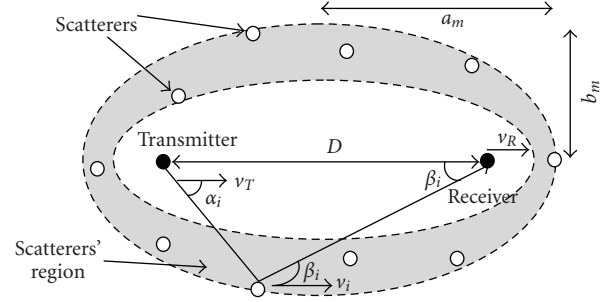


FIGURE 1: Proposed elliptical model.

3. Proposed Channel Model

The proposed channel model, shown in Figure 1, is based on the elliptical channel model first introduced in [2]. The original model was intended for modelling a mobile to basestation channel in a microcell, where the basestation is not very high as in macrocells and a line of sight may exist. Similar conditions are common in vehicular networks. The number and position of the surroundings depend on the terrain type. For highways, we expect a small number of surroundings; the scatterers increase as we approach the city where a large number of scatterers are more appropriate. The surroundings are placed uniformly within two ellipses. The parameters, a_m and b_m , of the outer ellipse are calculated from the delay spread using the following equations [6], while the inner ellipse is specified by the road geometries.

$$a_m = \frac{c\tau_m}{2},$$

$$b_m = \frac{1}{2}\sqrt{c^2\tau_m^2 - D^2}, \quad (2)$$

$$\tau_m = 3.244\sigma_t + \tau_0,$$

where τ_m is the maximum delay to be considered, σ_t is the delay spread, τ_0 is the minimum delay (line of sight delay), D is the distance between the transmitter and receiver, and c is the speed of light. The delay spread of VANET has been measured for various roads and traffic conditions in [9, 10]. The minimum mean delay spread measured was 103 nanoseconds. We adopt this value in our model as a worst-case scenario since a larger delay spread leads to smaller antenna correlation.

We assume that the existence of objects (cars) between the transmitter and receiver leads to blockage of line of sight. When a line of sight exists, a ground reflection is added if the distance between the transmitter and the receiver satisfies the following equation:

$$D \geq \frac{4\pi \cdot h_t \cdot h_r}{\lambda}, \quad (3)$$

where h_t and h_r are the heights of the transmitter and receiver antennas, respectively, and λ is the wavelength. The right-hand side of (3) is the minimum distance for the first Fresnel zone to touch the ground, and thus a ground reflection may exist only if (3) is satisfied [11, 12].

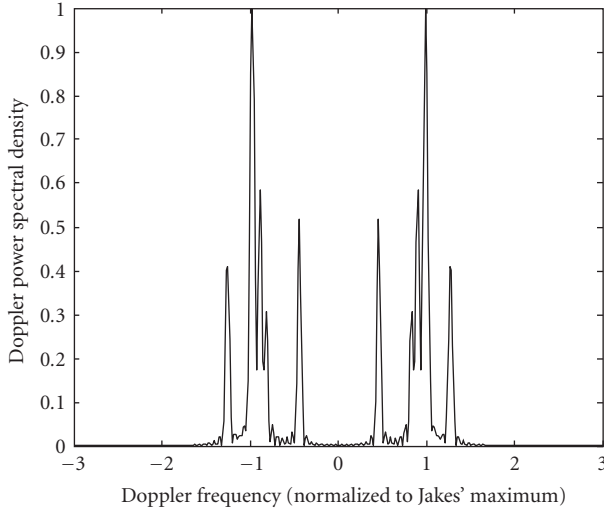


FIGURE 2: Channel autocorrelation function for proposed elliptical and Jakes' models.

The surroundings are not assumed fixed but their speeds are uniformly distributed between 0 and a maximum limit. For simplicity, we set the speed of the transmitter and surroundings relative to the speed of the receiver. Surroundings above the transmitter in Figure 1 are either fixed or moving in a direction opposite to the transmitter (negative speed) while those below the transmitter are either fixed or moving in the same direction as the transmitter (positive speed). It can be easily shown that the Doppler shift for any path (i) is given by (4) or (5) [13, 14]. Equation (5) follows from (4) since the last term in (4) is much smaller than the first. Considering the elliptical model in Figure 1, the maximum Doppler shift is no longer defined only by the relative speed of the transmitter/receiver ($v_T - v_R$) as in Jakes' model because the surroundings are not fixed [3, 14].

$$f_d(i) = f \left[\left(1 + \frac{v_T - v_i}{c} \cdot \cos(\alpha_i) \right) \cdot \left(1 + \frac{v_i - v_R}{c} \cdot \cos(\beta_i) \right) \right] - f, \quad (4)$$

$$f_d(i) = \frac{f}{c} [(v_T - v_i) \cdot \cos(\alpha_i) + (v_i - v_R) \cdot \cos(\beta_i)] + \frac{f}{c^2} (v_T - v_i)(v_i - v_R) \cos(\alpha_i) \cos(\beta_i), \quad (5)$$

The channel response ($h(t)$) at time (t) can be represented by

$$h(t) = \sum_{i=0}^N g_i \cdot \exp \left(j \left\{ \frac{2\pi \cdot f_d(i) \cdot t}{c} + \theta_i + \varphi_i \right\} \right) \cdot u(t - t_i), \quad (6)$$

where g_i is the reflection coefficient, t_i and θ_i are the excess distance delay and phase, respectively, φ_i is a random phase, N is the number of paths, and $u(t)$ is the unit step function. The line of sight is represented by the $i = 0$ term.

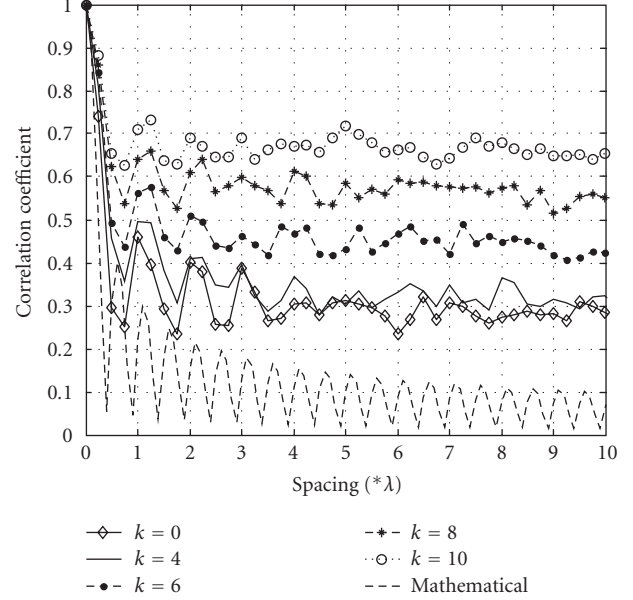


FIGURE 3: Antenna correlation versus spacing for sample line of sight strengths, with ground reflection.

4. Model Statistics and Antenna Correlation

For our simulations, we use 10 scatterers. The maximum speed was set to 120 km/h with the transmitter moving at 90 km/h and fixed receiver. The ratio of the line of sight component to any of the other scatters is equal to k . The delay spread is 103 nanoseconds as measured in [9]. The distance (D) between the transmitter and receiver is 1 km, which is the maximum transmission range specified for IEEE 802.11p [15], and the heights of the antennas were set to 1.5 m. The frequency is 5.9 GHz as specified by ASTM [16]. The amplitude distribution of the received signal using our model was found to follow Rayleigh distribution for no line of sight and Rician distribution when a line of sight component exists. This agrees with the statistics obtained from measurements in [11, 17]. The Rician distribution can be approximated by a Gaussian distribution under strong line of sight conditions [4].

The Doppler spectrum is shown in Figure 2. Comparing Figure 2 with the classical Jakes spectrum [3], we observe that the maximum Doppler shift exceeds that suggested by Jakes due to the movement of the scatterers. In Jakes' Doppler spectrum, the spectrum is bounded by f_d given in (1), whereas in VANET, the spectrum extends beyond this value as observed from Figure 3. This effect appears in the autocorrelation function as faster variation compared to that of Jakes' model. Both models give identical results if the speeds of the scatterers are set to zero. Similar conclusions were reached in [18] via measurements.

The correlation between two antennas (ρ_{ij}) can be calculated theoretically for Rayleigh fading using the AOA probability distribution $p(\alpha)$ and the equation [19]

$$\rho_{ij} = \int_0^{2\pi} e^{j(2\pi/\lambda)d \cos(\varphi - \psi)} \cdot p(\varphi) \cdot d\varphi, \quad (7)$$

where d is the spacing between the antennas and ψ is the angle of orientation of the array (set to $\pi/2$ for broadside and 0 for end fire). For mobile terminals, the surroundings are usually assumed to be uniformly distributed in a circle around the terminal (Lee's model) leading to the AOA distribution of the following equation [19]:

$$p(\varphi) = \begin{cases} \frac{1}{2\pi}, & 0 \leq \varphi \leq 2\pi, \\ 0, & \text{otherwise.} \end{cases} \quad (8)$$

Figure 3 compares the correlation between the antennas under various line of sight strengths and no line of sight conditions using the elliptical model with the correlation from (7). As can be seen, (7) gives an optimistic estimate of the correlation due to the assumption of uniform angle distribution which is realistic only in rich scattering channels. We also note that the correlation increases as the line of sight strength increases since the received signal becomes dominated by the line of sight component. The ground reflection reduces the correlation since the attenuation for line of sight is inversely proportional to D^4 instead of D^2 , thus the contribution of line of sight is reduced [11, 12]. Without ground reflection, the correlation becomes higher, and it is not possible to reduce it unless very large, impractical antenna spacings are used.

Although the line of sight condition is ideal for single antenna systems, it can lead to severe degradation in the performance of BLAST systems [19–21]. To illustrate this, we used the channel model without ground reflection to simulate a 2×4 VBLAST system using PSK modulation, 1 MHz bandwidth, and perfect channel knowledge. As shown in Figure 4, the performance drops as the line of sight increases. This is due to the correlation between the antennas which leads to the loss of the diversity since the antennas receive similar signals. In the next section, we introduce the proposed channel update algorithm.

5. Channel Update

The performance of MIMO systems depends on the accuracy of channel state information (CSI). In a fast varying channel, the channel estimate must be updated more frequently. Generally, a training sequence is used for channel estimation [22–24]; however under fast varying conditions, the interval between successive training sequences becomes small, and thus the efficiency is reduced. Our aim in this section is to develop an algorithm to update the channel estimate using the received signal in order to increase the interval between successive training intervals.

Several channel tracking algorithms are available for single and multiple antenna systems. In [25], a maximum likelihood channel tracking algorithm has been proposed. Kalman filters have been considered in several papers. In [26], the authors combined a Kalman filter with a decision feedback equaliser (DFE). The DFE is used to estimate the transmitted signal, and its output is fed to the Kalman filter for channel tracking. In [27], an autoregressive moving average (ARMA) filter was used to model the channel

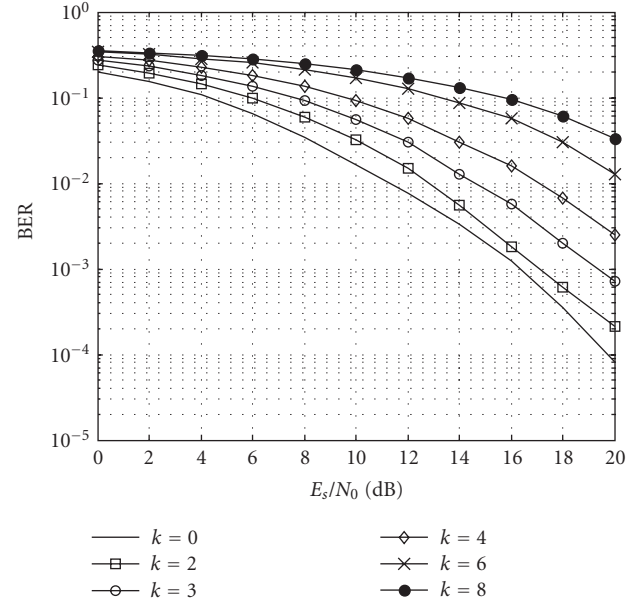


FIGURE 4: Performance of VBLAST for various line of sight strengths.

response based on Jakes' channel power spectral density; this was then used to design a Kalman filter for tracking. The main limitation of these algorithms is complexity. The decoding algorithms for MIMO systems are usually very complicated and, therefore, it is desirable to minimise the channel estimation and tracking complexity. In this section, we develop a simple single tap Kalman filter to update the channel and thus reduce the BER while keeping the increase in hardware complexity to minimum.

For a $p \times q$ VBLAST system with p transmit and q receive antennas, $q \geq p$, in a flat fading channel, the received signal vector of length q (\mathbf{r}_{n-1}) at time index $n-1$ can be written as

$$\mathbf{r}_{n-1} = \mathbf{H}_{n-1} \mathbf{s}_{n-1} + \mathbf{m}_{n-1}, \quad (9)$$

where \mathbf{H}_{n-1} is the $q \times p$ channel matrix, \mathbf{s}_{n-1} is the column vector of p transmitted symbols, and \mathbf{m}_{n-1} is the column vector of q white noise samples at time $n-1$. Unless otherwise specified, bold upper-case characters represent matrices and bold lower-case characters represent vectors while normal lower-case characters represent elements within the matrix/vector of the same character. Our analysis assumes that the antenna separation is large enough for the received signals to be uncorrelated.

Let the estimated channel matrix be $\hat{\mathbf{H}}_{n-1}$. The simplest BLAST receiver (zero-forcing receiver) calculates an estimate of the transmitted symbols ($\hat{\mathbf{s}}_{n-1}$) using the pseudoinverse of the channel matrix ($\hat{\mathbf{H}}_{n-1}^+$) as [28]

$$\hat{\mathbf{s}}_{n-1} = \hat{\mathbf{H}}_{n-1}^+ \times \mathbf{r}_{n-1}. \quad (10)$$

Define $\Delta \mathbf{H}_n$ as

$$\Delta \mathbf{H}_n = (\mathbf{r}_{n-1} - \hat{\mathbf{H}}_{n-1} \hat{\mathbf{s}}_{n-1}) \times \hat{\mathbf{s}}_{n-1}^+. \quad (11)$$

Substituting (9) in (11) and assuming correct decoding, we find

$$\Delta \mathbf{H}_n = (\mathbf{H}_{n-1} - \hat{\mathbf{H}}_{n-1}) \times \mathbf{s}_{n-1} \mathbf{s}_{n-1}^+ + \mathbf{m}_{n-1} \mathbf{s}_{n-1}^+. \quad (12)$$

Note that the term $(\mathbf{r}_{n-1} - \hat{\mathbf{H}}_{n-1} \hat{\mathbf{s}}_{n-1})$ is calculated in the cancellation step of the VBLAST decoding algorithm. $\Delta \mathbf{H}_n$ can be used with a first-order Kalman [13] filter to improve the channel estimation as

$$\hat{\mathbf{H}}_n = \hat{\mathbf{H}}_{n-1} + \mathbf{K} \cdot \Delta \mathbf{H}_n, \quad (13)$$

where \mathbf{K} is a $q \times p$ matrix of update parameters and the dot in (13) represents the element-by-element multiplication.

We now need to find the optimum value of \mathbf{K} , however, since we assume that the receive antennas are not correlated; we need to optimise for only one antenna. Equation (12) can be rewritten for the elements of the matrix $\Delta \mathbf{H}_n$ as

$$\Delta h_{ij}^n = \left(r_i^{n-1} - \sum_{l=1}^p \hat{h}_{il}^{n-1} \cdot \hat{s}_l^{n-1} \right) a_j^{n-1}. \quad (14)$$

The subscripts identify the row (i) and column (j or l) which represent receive and transmit antennas, respectively, while the superscript (n) denotes the time index. a_j is the element at column j of the row vector $(\hat{\mathbf{s}}^+)$. Equation (14) can be expanded using (9) as

$$\Delta h_{ij}^n = \left(\sum_{l=1}^p (h_{il}^{n-1} \cdot s_l^{n-1} - \hat{h}_{il}^{n-1} \cdot \hat{s}_l^{n-1} + m_i^{n-1}) \right) a_j^{n-1}, \quad (15)$$

and assuming correct decoding as

$$\begin{aligned} \Delta h_{ij}^n &= \left(\sum_{l=1}^p (h_{il}^{n-1} - \hat{h}_{il}^{n-1}) \cdot s_l^{n-1} \right) a_j^{n-1} + m_i^{n-1} a_j^{n-1} \\ &= \beta \varepsilon_{ij}^{n-1} + \sum_{\substack{l=1 \\ l \neq j}}^p \varepsilon_{il}^{n-1} \cdot s_l^{n-1} \cdot a_j^{n-1} + m_i^{n-1} a_j^{n-1}. \end{aligned} \quad (16)$$

Here, $\varepsilon_{ij}^{n-1} = h_{ij}^{n-1} - \hat{h}_{ij}^{n-1}$, and β is the product of the s_j^{n-1} and a_j^{n-1} terms. The elements of the updated channel can be written as

$$\hat{h}_{ij}^n = \hat{h}_{ij}^{n-1} + k_{ij} \Delta h_{ij}^n, \quad (17)$$

$$\hat{h}_{ij}^n = \hat{h}_{ij}^{n-1} + \beta k_{ij} \varepsilon_{ij}^{n-1} + k_{ij} \sum_{\substack{l=1 \\ l \neq j}}^p \varepsilon_{il}^{n-1} s_l^{n-1} a_j^{n-1} + k_{ij} m_i^{n-1} a_j^{n-1}. \quad (18)$$

With the assumption of independent identically distributed (i.i.d) white data and equal average signal to noise ratio (SNR) for the receive antennas, the last two terms in (18) can be approximated by white noise with average power [13]:

$$\bar{N}_{0,j} = \frac{P_0}{\rho_j} \left(1 + \sum_{\substack{l=1 \\ l \neq j}}^p e_l \right), \quad (19)$$

where P_0 is the original noise to signal power ratio for receive antenna i , e_l is the average error covariance reduction value, and ρ_j is a constant that specifies the fraction of noise associated with stream j . The optimum value of k_{ij} is the one that minimises the expression $E[|h_{ij}^n - \hat{h}_{ij}^n|^2]$. For $f_D T_s < 0.2$, T_s is the symbol duration, the channel autocorrelation function ($A(mT_s)$) can be approximated by (20) [29, 30]. The optimum value of k_{ij} is then found using (21) to (24),

$$A(mT_s) \approx 1 - \pi^2 f_D^2 T_s^2 \cdot m^2, \quad (20)$$

$$k_{ij} = k_j \quad \forall i, \quad (21)$$

$$k_j = 3.6 \times \sqrt[3]{\frac{\rho_j (f_D T_s)^2}{\beta P_0 (1 + \sum_{l=1, l \neq j}^p e_l)}} \quad (22)$$

$$= 3.6 \times \sqrt[3]{\frac{(f_D T_s)^2}{P_0 (1 + \sum_{l=1, l \neq j}^p e_l)}},$$

$$e_j \approx \frac{0.75}{p} k_j, \quad (23)$$

$$P_0 = \frac{1}{E_s/N_0}. \quad (24)$$

We define E_s/N_0 as the total SNR if all transmitting antennas transmit the same symbol. We set β and ρ_j equal to $1/p$ in (22) since we assume equal average transmit (receive) power for each transmit (receive) antenna. The k_j parameters are calculated recursively. First, we assume no interference from the other symbols and set $e_j = 0$. This is best suited for the last decoded symbol in VBLAST since all the other symbols would be cancelled out by then. We then calculate k_j and e_j for this stream. Next, we substitute the new value of e_j for the next to last decoded symbol and calculate the k_j then update e_j . After all the initial k_j parameters are calculated, the process is repeated again with e_j from the calculated k_j . This process converges very quickly, and the final values of k_j are not very different from the initial ones. The parameters then can be used to update the channel estimate. The algorithm requires the calculation of $p k_j$ parameters, one for each transmit antenna (21) and (24). These can be calculated once at the beginning of the packet and held constant for the duration of the packet. $\Delta \mathbf{H}_n$ requires the pseudoinverse of the $(p \times 1)$ vector \mathbf{s} , which can be precalculated and stored, and then multiplying it by the term $(\mathbf{r}_{n-1} - \hat{\mathbf{H}}_{n-1} \hat{\mathbf{s}}_{n-1})$, (11), which is calculated in the VBLAST algorithm. This multiplication consists of $p \times q$ complex multiplication. The update algorithm, (13), requires $p \times q$ real-by-complex multiplication and $p \times q$ complex addition.

A simple analysis shows that the algorithm requires $6p \times q$ real multiplications and $4p \times q$ real additions per update. Assuming a 2×4 system, the algorithm then requires 48 multiplications and 32 additions. If channel update is conducted for every symbol, then a chosen 500 MHz DSP processor, which executes a multiplication in 1 cycle, can compute the update in 160 nanoseconds.

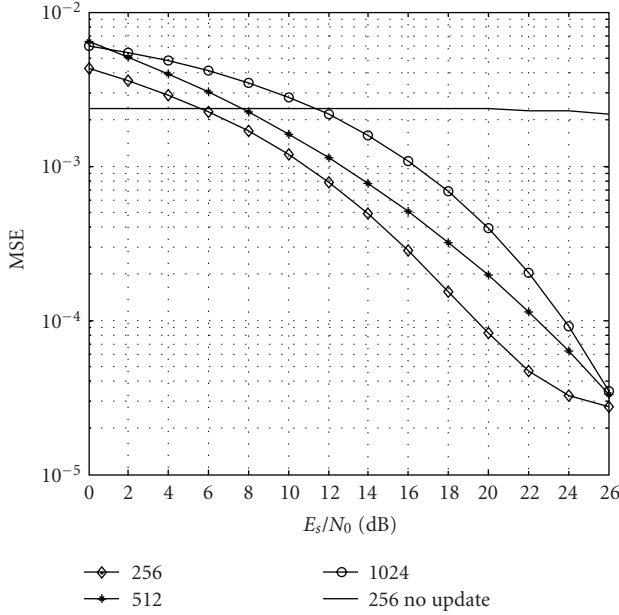


FIGURE 5: MSE of channel estimation for 180 km/h.

We ran a number of simulations using Matlab for a 2×4 VBLAST system with a symbol rate of 1 MSymbol/s and the elliptical channel model. The frequency was 5.9 GHz. In our simulations, initially the algorithm would have perfect channel knowledge rather than estimating from a training sequence. This is necessary to isolate any errors that might arise from the use of training sequence estimation. The initial values of k_j were used to reduce complexity, and the channel estimate was updated for every symbol.

Figure 5 shows the mean square error in the estimated channel for the cases of 256, 512, and 1024 symbols per antenna using QPSK modulation with channel update, using (12) and from (21) to (24), compared to 256 without update. As can be seen from Figure 5, the update algorithm reduces the MSE by 50% at 12 dB E_s/N_0 . The MSE in Figure 5 without update does not depend on the SNR because the receiver is assumed to have perfect noise-free estimate of the channel at the beginning of the packet, and this is held constant for the duration of the packet. Figure 6 shows the MSE versus the symbol number for 26 dB E_s/N_0 . Initially, the receiver will have perfect channel knowledge ($MSE \approx 0$) but with time this estimate becomes invalid due to the high Doppler shift. If a training sequence was used, the initial MSE will be greater than 0, thus shifting the curves upwards. The difference between the curves, however, will not change and, therefore, the MSE comparison will still hold.

Figure 7 shows the BER performance of QPSK for various relative vehicle speeds. As can be seen, the performance improves considerably when the algorithm is used and is 2 dB from that of perfect channel knowledge for 60 km/h. Figure 8 shows the performance of the same system using QPSK with various packet lengths for a speed of 60 km/h.

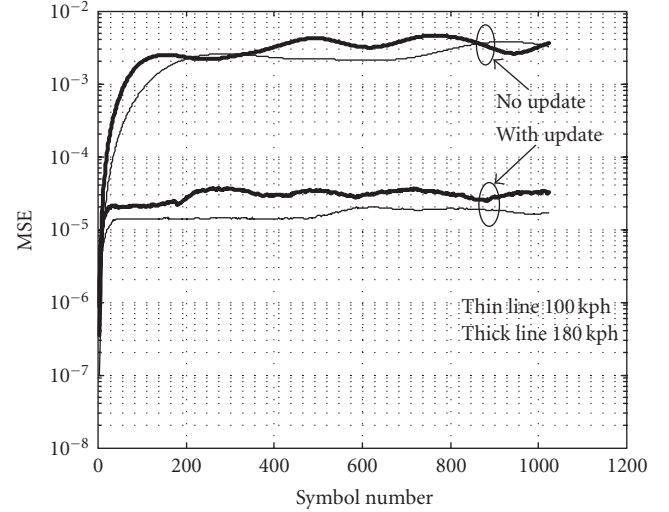


FIGURE 6: MSE of channel estimation versus the number of symbols at 26 dB.

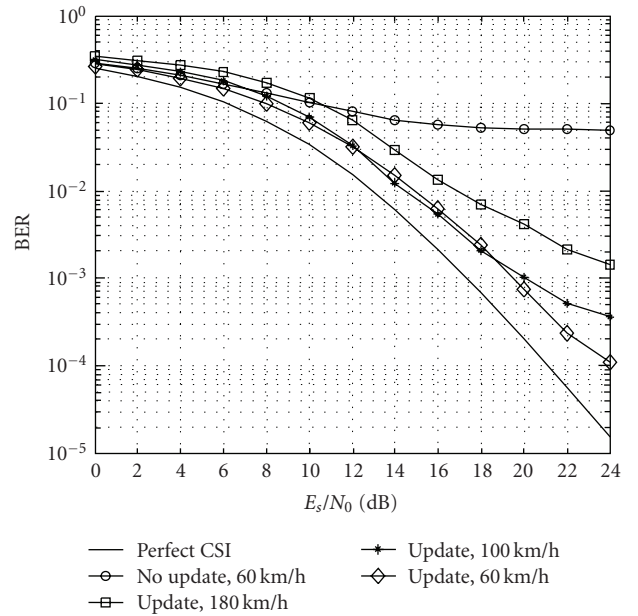


FIGURE 7: QPSK BER with and without channel update.

From Figure 8, we observe that the performance degrades as the packet length increases; this is due to two reasons. The first reason is estimation error, as the estimation process proceeds, the error in the estimation accumulates, and for long packets this will lead to erroneous results near the end of the packet. The second reason is detection errors since the probability of symbol errors increases as the packet length increases. The estimation algorithm assumes correct decoding; therefore, such errors will affect the performance of the algorithm.

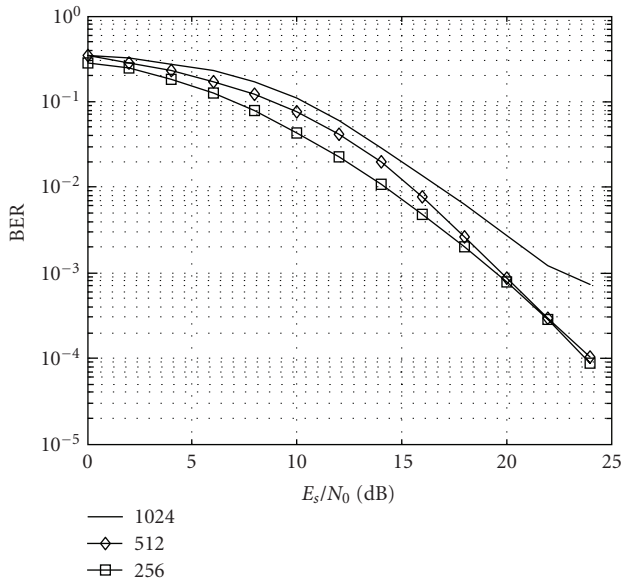


FIGURE 8: BER for different packet sizes, 60 km/h.

6. Conclusion

In this paper, we introduced a channel model for vehicular networks. The model was compared to Jakes' model, and it was shown that the Doppler power spectrum extends beyond Jakes' maximum frequency due to the movement of the surroundings, transmitter, and receiver. The correlation between antennas was then studied, and the results show that under very strong line of sight conditions, the correlation is high and, therefore, a small gain is expected from the use of multiple antennas while for moderate and no line of sight conditions the correlation is low. We also developed a simple recursive algorithm to keep track of changes in the channel and update the channel estimation matrix for VBLAST. The update algorithm enhances the channel estimation on a symbol-by-symbol basis, but this can be relaxed for high symbol rates and/or slow fading as the channel coherence time will be large compared to the symbol duration. The proposed algorithm improves system BER and channel estimate MSE via continuous and accurate channel updating and has less computational complexity compared to existing tracking algorithms as a result of using a simplified Kalman filter. Simulation results showed remarkable improvements when using the update algorithm compared to the training of only channel estimation. The algorithm is capable of updating the channel estimation for VBLAST for nodes moving at high speeds thus improving the bit error rate and reliability of VANET.

Acknowledgment

The authors would like to thank France Telecom and the University of Plymouth for supporting this work as well as the anonymous reviewers for their valuable comments.

References

- [1] S. Haykin and M. Moher, *Modern Wireless Communications*, Prentice-Hall, Upper Saddle River, NJ, USA, 2005.
- [2] J. C. Liberti and T. S. Rappaport, "A geometrically based model for line-of-sight multipath radio channels," in *Proceedings of the 46th IEEE Vehicular Technology Conference (VTC '96)*, vol. 2, pp. 844–848, Atlanta, Ga, USA, April-May 1996.
- [3] W. C. Jakes, *Microwave Mobile Communications*, IEEE Press, Piscataway, NJ, USA, 1994.
- [4] J. D. Parsons, *The Mobile Radio Propagation Channel*, John Wiley & Sons, New York, NY, USA, 2001.
- [5] W. C. Y. Lee, *Mobile Communications Engineering*, McGraw-Hill, New York, NY, USA, 1982.
- [6] R. B. Ertel, P. Cardieri, K. W. Sowerby, T. S. Rappaport, and J. H. Reed, "Overview of spatial channel models for antenna array communication systems," *IEEE Personal Communications*, vol. 5, no. 1, pp. 10–22, 1998.
- [7] C. S. Patel, G. L. Stüber, and T. G. Pratt, "Simulation of Rayleigh-faded mobile-to-mobile communication channels," *IEEE Transactions on Communications*, vol. 53, no. 11, pp. 1876–1884, 2005.
- [8] A. G. Zajić and G. L. Stüber, "A three-dimensional MIMO mobile-to-mobile channel model," in *Proceedings of the IEEE Wireless Communications and Networking Conference (WCNC '07)*, pp. 1885–1889, Hong Kong, March 2007.
- [9] D. W. Matolak, I. Sen, W. Xiong, and N. T. Yaskoff, "5 GHz wireless channel characterization for vehicle to vehicle communications," in *Proceedings of IEEE Military Communications Conference (MILCOM '05)*, vol. 5, pp. 3022–3016, Atlantic City, NJ, USA, October 2005.
- [10] A. Paier, J. Karedal, N. Czink, et al., "Car-to-car radio channel measurements at 5 GHz: pathloss, power-delay profile, and delay-Doppler spectrum," in *Proceedings of 4th IEEE International Symposium on Wireless Communication Systems (ISWCS '07)*, pp. 224–228, Trondheim, Norway, October 2007.
- [11] L. Cheng, B. E. Henty, D. D. Stancil, F. Bai, and P. Mudalige, "Mobile vehicle-to-vehicle narrow-band channel measurement and characterization of the 5.9 GHz dedicated short range communication (DSRC) frequency band," *IEEE Journal on Selected Areas in Communications*, vol. 25, no. 8, pp. 1501–1516, 2007.
- [12] A. Polydoros, K. Dessouky, J. M. N. Pereira, et al., "Vehicle to roadside communications study," Research Reports UCB-ITS-PRR-93-4, California Partners for Advanced Transit and Highways (PATH), University of California, Berkeley, Calif, USA, June 1993.
- [13] F. T. Ulaby, *Fundamentals of Applied Electromagnetics*, Prentice-Hall, Upper Saddle River, NJ, USA, 1999.
- [14] T. P. Gill, *The Doppler Effect*, Logos Press, New York, NY, USA, 1965.
- [15] IEEE Draft P802.11p/D2.0, November 2006.
- [16] American Society for Testing and Materials (ASTM), <http://www.astm.org/>.
- [17] J. Maurer, T. Fügen, and W. Wiesbeck, "Narrow-band measurement and analysis of the inter-vehicle transmission channel at 5.2 GHz," in *Proceedings of the 55th IEEE Vehicular Technology Conference (VTC '02)*, vol. 3, pp. 1274–1278, Birmingham, Ala, USA, May 2002.
- [18] L. Cheng, B. E. Henty, D. D. Stancil, and F. Bai, "Doppler component analysis of the suburban vehicle-to-vehicle DSRC propagation channel at 5.9 GHz," in *Proceedings of the IEEE Radio and Wireless Symposium (RWS '08)*, pp. 343–346, Orlando, Fla, USA, January 2008.

- [19] D. Chizhik, F. Rashid-Farrokhi, J. Ling, and A. Lozano, "Effect of antenna separation on the capacity of BLAST in correlated channels," *IEEE Communications Letters*, vol. 4, no. 11, pp. 337–339, 2000.
- [20] D. Chizhik, G. J. Foschini, M. J. Gans, and R. A. Valenzuela, "Keyholes, correlations, and capacities of multielement transmit and receive antennas," *IEEE Transactions on Wireless Communications*, vol. 1, no. 2, pp. 361–368, 2002.
- [21] X. Li and Z. Nie, "Performance losses in V-BLAST due to correlation," *IEEE Antennas and Wireless Propagation Letters*, vol. 3, no. 1, pp. 291–294, 2004.
- [22] M. Biguesh and A. B. Gershman, "Training-based MIMO channel estimation: a study of estimator tradeoffs and optimal training signals," *IEEE Transactions on Signal Processing*, vol. 54, no. 3, pp. 884–893, 2006.
- [23] H. Minn and N. Al-Dhahir, "Optimal training signals for MIMO OFDM channel estimation," *IEEE Transactions on Wireless Communications*, vol. 5, no. 5, pp. 1158–1168, 2006.
- [24] B. Park and T. F. Wong, "Optimal training sequence in MIMO systems with multiple interference sources," in *Proceedings of the IEEE Global Telecommunications Conference (GLOBECOM '04)*, vol. 1, pp. 86–90, Dallas, Tex, USA, November–December 2004.
- [25] E. Karami and M. Shiva, "Maximum likelihood MIMO channel tracking," in *Proceedings of the 59th IEEE Vehicular Technology Conference (VTC '04)*, vol. 2, pp. 876–879, Milan, Italy, May 2004.
- [26] G. Yanfei and H. Zishu, "MIMO channel tracking based on Kalman filter and MMSE-DFE," in *Proceedings of the International Conference on Communications, Circuits and Systems (ICCCAS '05)*, vol. 1, pp. 223–226, Hong Kong, May 2005.
- [27] L. Li, H. Li, H. Yu, B. Yang, and H. Hu, "A new algorithm for MIMO channel tracking based on Kalman filter," in *Proceedings of the IEEE Wireless Communications and Networking Conference (WCNC '07)*, pp. 164–168, Hong Kong, March 2007.
- [28] D. Gore, R. W. Heath Jr., and A. Paulraj, "On performance of the zero forcing receiver in presence of transmit correlation," in *Proceedings of IEEE International Symposium on Information Theory (ISIT '02)*, p. 159, Lausanne, Switzerland, June–July 2002.
- [29] H. Meyr, M. Moeneclaey, and S. A. Fechtel, *Digital Communication Receivers*, John Wiley & Sons, New York, NY, USA, 1998.
- [30] T. Wang, J. G. Proakis, E. Masry, and J. R. Zeidler, "Performance degradation of OFDM systems due to doppler spreading," *IEEE Transactions on Wireless Communications*, vol. 5, no. 6, pp. 1422–1432, 2006.